A GENUINELY MULTIDISCIPLINARY JOURNAL

CHEMPLUSCHEM

CENTERING ON CHEMISTRY

Accepted Article

Title: A New Cerium-Containing Metal-Organic Framework: Synthesis and Heterogeneous Catalytic Activity toward Fenton-Like Reactions

Authors: Thanh Truong, Giao H. Dang, Y B. N. Tran, Toan V. Pham, Vu T. Pham, Nhu T. H. Luu, Hieu D. Nguyen, Phuong T. K. Nguyen, and Huong T. D. Nguyen

To be cited as: *ChemPlusChem* 10.1002/cplu.201900325

Link to VoR: http://dx.doi.org/10.1002/cplu.201900325

A Journal of ChemPubSoc Europe

WILEY-VCH

www.chempluschem.org

A New Cerium-Containing Metal-Organic Framework: Synthesis and Heterogeneous Catalytic Activity toward Fenton-Like Reactions

Dr. Giao H. Dang,[a] Dr. Y B. N. Tran,[b] Dr. Toan V. Pham,[a] Vu T. Pham,[c] Nhu T. H. Luu,[c] Hieu D. Nguyen,[c] Dr. Phuong T. K. Nguyen,[b] Dr. Huong T. D. Nguyen,[*,d] Prof. Thanh Truong[*,c]

[a] College of Engineering Technology, Can Tho University, 3/2 Street, Ninh Kieu District, Can Tho City, Viet Nam

[b] Center for Innovative Materials and Architectures (INOMAR), VNU-HCM,
Quarter 6, Linh Trung Ward, Thu Duc District, Ho Chi Minh City, Viet Nam

[c] Department of Chemical Engineering, Ho Chi Minh University of Technology, VNU-HCM,
268 Ly Thuong Kiet, District 10, Ho Chi Minh City, Viet Nam

[d] Department of Chemistry, University of Science, VNU-HCM,
227 Nguyen Van Cu, District 5, Ho Chi Minh City, Viet Nam

[*]Email: tvthanh@hcmut.edu.vn and ntdhuong@hcmus.edu.vn

Ph: (+84 28) 38647256 ext. 5681 Fx: (+84 8) 38637504

ABSTRACT

A new cerium-based metal–organic framework, namely MOF-589, was synthesized using tetracarboxylic acid, benzoimidephenanthroline tetracarboxylic acid (H_4BIPA-TC), as organic linker. Full characterization including single crystal and powder X-ray diffraction analysis, thermogravimetrical analysis, scanning electron microscopy, and N_2 adsorption measurement at low pressure and 77 K were demonstrated. The material was employed as an efficient heterogeneous catalyst for decomposition of methylene blue (MB) dye (40 ppm) in the presence of H_2O_2 in 15 minutes. Interestingly, comparison study was conducted and the activity of MOF 589 was higher than that of other iron-based heterogeneous and cerium-based catalysts. Further experiments on clarification of MOF 589 activity indicated that BIPA-TC linker might have an important impact via cooperative effect on metal cluster. Control studies confirmed the necessity of catalyst and its recyclability. In particular, catalysis from leached

cerium in reaction filtrate is unlikely and the solid material could be reused at least 08 times without remarkable loss in activity.

INTRODUCTION

Textile industries utilized about 65 % of approximately million tons of dyestuffs are annually manufactured.[1] The inefficiency of dyeing process resulted in the production of large amount of contaminated wastewater effluent.[2-3] These dyes present significant environmental problems due to their non-biodegradation and toxicity to aquatic animals and plant.[4-5] Therefore, numerous treatments including physical, mechanical, biological, and chemical methods were investigated to remove these undesirable compounds.[6-10] Fenton or Fenton-like process as one of the most effective advanced oxidation processes (AOPs) is of common interest and has shown great potential.[11-13] The processes involve the simple generation of highly active hydroxyl radical by reacting inexpensive and environmental benign H_2O_2 with a transition metal, especially with iron ions.[14-15] In addition, copper, cadmium, chromium, mercury, nickel, and vanadium have also been shown to produce reactive radicals in the presence of hydrogen peroxide.[16] However, the homogeneous protocols suffer the large sludge formation and the requirement of acidic solution. [11] Thus, heterogeneous systems have been sought as more practical and efficient alternatives by overcoming the aforementioned drawbacks in conjunction with their recyclability. Recently, several studies on heterogeneous Fenton processes have been reported and most of catalytic systems consist of Fe ions.[17-18] The catalysts containing cerium, the most abundant of the rare earth metals, for radical production in the presence of hydrogen peroxide via Fenton-type mechanism have been disclosed.[19-21] The proposed mechanism invovled the Ce^{3+}/Ce^{4+} catalytic cycle while Ce^{3+} promote •OH production in a Fenton system.[22] Most of reported studies utilized nanoceria CeO_2 or cerium (III) salts. Therefore, the development of new catalytic protocol would provide more insights of reactions from mechanistic viewpoint.

Metal–organic frameworks (MOFs) are porous crystalline compounds that combine metal ions or metal-containing clusters (termed as secondary building units, SBUs) with rigid organic linkers-have emerged as an important class of porous materials.[23] The designable linkers and the variety of inorganic metal nodes allows for the synthesis of numerous fascinating MOFs with many applications, including gas storage, separation, catalysis, sensors, drug delivery and biomedical imaging.[24-29] Compared with MOFs based on d-block transition metal ions, lanthanides-based MOFs (Ln-MOFs) have been far less studied. Lanthanide ions have high coordination numbers and flexible connectivities, in range of 6-12, due to their large ionic radii. [30] As a result, most of Ln-MOFs frameworks are condensed and less porous. Their network topologies are also hard to control. However, lanthanide ions have 4-f electron configurations, which lead to the resulting Ln-MOFs with unique magnetic [31-33] and photophysical properties.[34-36] Particularly, cerium metal, as an inexpensive rare earth element, has $4f^1 5d^1 6s^2$ electron configuration. Recently, cerium-based organic frameworks have been reported and utilized in various redox application.[25, 37-39] Through the allowed d-f transitions, Ce(III) ion can emit intense broadband emission which depends on the linker coordination.[40] By taking advantage of this, we herein present a novel Ce-MOF using benzoimidephenanthroline tetracarboxylic acid as linker and its heterogeneous catalytic activity in Fenton-like reaction. Remarkably, preliminary results indicated that π-π stacking within organic linker plays an important role in activity of the Ce-MOF.

RESULTS AND DISCUSSION

Crystal structures of MOF-589

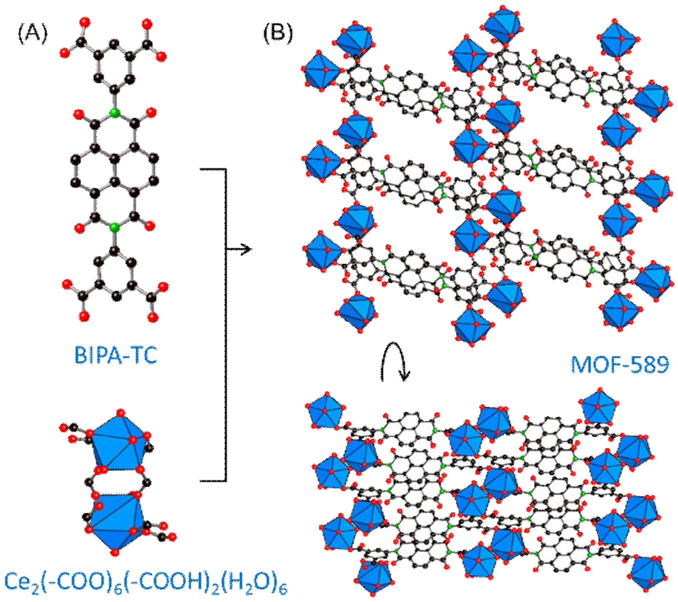

Figure 1. Crystal structure of MOF-589. (a) Linking of BIPA-TC and [Ce_2(-COO)$_6$(-COOH)$_2$(H_2O)$_6$] SBUs result in (b) MOF-590. Atom colors: Ce, blue polyhedra; C, black; O, red; N, green. All H atoms are omitted for clarity.

The ToposPro (v.5.3) software program was employed to simplify the structures of MOF-589 and to classify the underlying net.[42] The tetratopic linker was considered as two triangular nodes. SCXRD analysis indicates that MOF-589 crystallizes in the triclinic *P*-1 space group (No. 2) with lattice parameters a = 8.4259(4) Å, b = 11.4299(6) Å, c = 17.9923(9) Å, α = 93.349(2)°, β = 95.926(2)°, and γ = 107.913(2)°. Its asymmetric unit contains one crystallographically independent Ce(III) ion, one partially deprotonated HBIPA-TC^{3-} ligand and three coordinated water molecules. The framework of MOF-589 is composed of dinuclear [Ce_2(-COO)$_6$(-COOH)$_2$(H_2O)$_6$] SBUs, a Ce^{3+} cation is seen with a coordination number of eight. Two carboxylate functionalities coordinate in a bridging fashion to two Ce cations, four carboxylate and two carboxylic acid functionalities in monodentate type. The coordination environment is completed by six additional water ligands (Figure 1 and Figure 2).

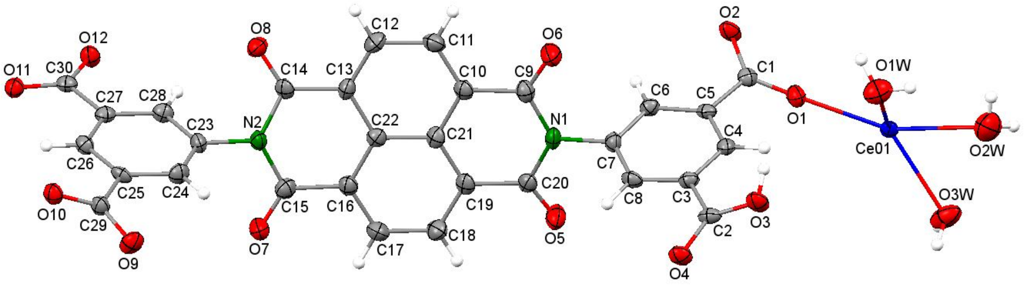

Figure 2. Representation of the asymmetric unit for MOF-589 material. Atoms: Ce in blue; C in gray; O in red; N in dark blue and protons in white. Ellipsoids are displayed at the 75% probability level. CCDC 1843313 contains the supplementary crystallographic data for this paper. These data can be obtained free of charge from The Cambridge Crystallographic Data Centre.

Due to the distance of 3.0 Å between two closest planar naphthalene diimide moieties, two neighboring BIPA-TC ligand could` have π−π interactions between the conjugated π-deficient naphthalene diimide rings. Along the *a*-axis, MOF-589 displays parallelogram 1D channels, which have window size of 3.3 x 11.4 Å^2. It is noted that all channels and pores are blocked along the *b* and *c*-axis (**Figure 1b**). The void space of MOF-589, in fully desolvated form, is

~20.8% per PLATON calculations and the pore volume is 0.13 cm^3g^{-1}.[43] Topological analysis reveals that the three-dimensional framework of MOF-589 adopts sqc495 topology with a point symbol of $(4.6^2)_4(4^4.6^8.8^{12}.10^4)$ due to the linkage of one distinct type of 8-c inorganic SBUs and one distinct type of 3-c linker (**Figure 3**).[44]

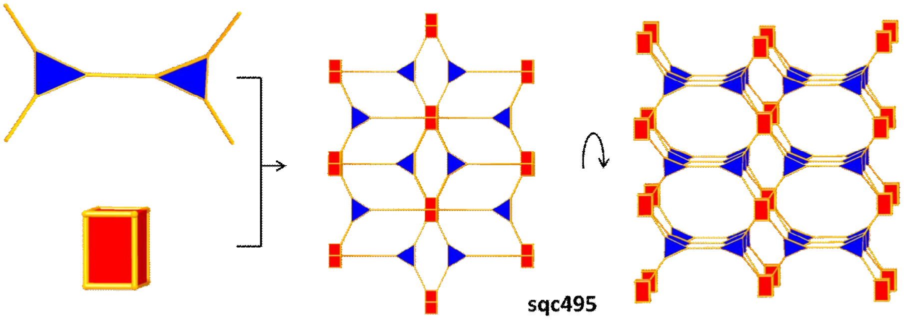

Figure 3. The structure of MOF-589 adopts the sqc495 topology

Other structural characterization and porosity properties

Phase purity of MOF-589 was confirmed by PXRD analysis of the as-synthesized materials in comparison with the respective pattern calculated from the crystal structures (Figure 4a). In turn, the as-synthesized MOF-589 were washed with DMF to remove unreacted species and subsequently solvent-exchanged with EtOH. To obtain desolvated materials, occluded solvent molecules were removed under reduced pressure at room temperature for 24 h, followed by heating at 60 °C for 24 h. Structural maintenance after activation was proven by PXRD analysis, in which the peak positions of the activated samples were coincident to both the as-synthesized and calculated patterns.

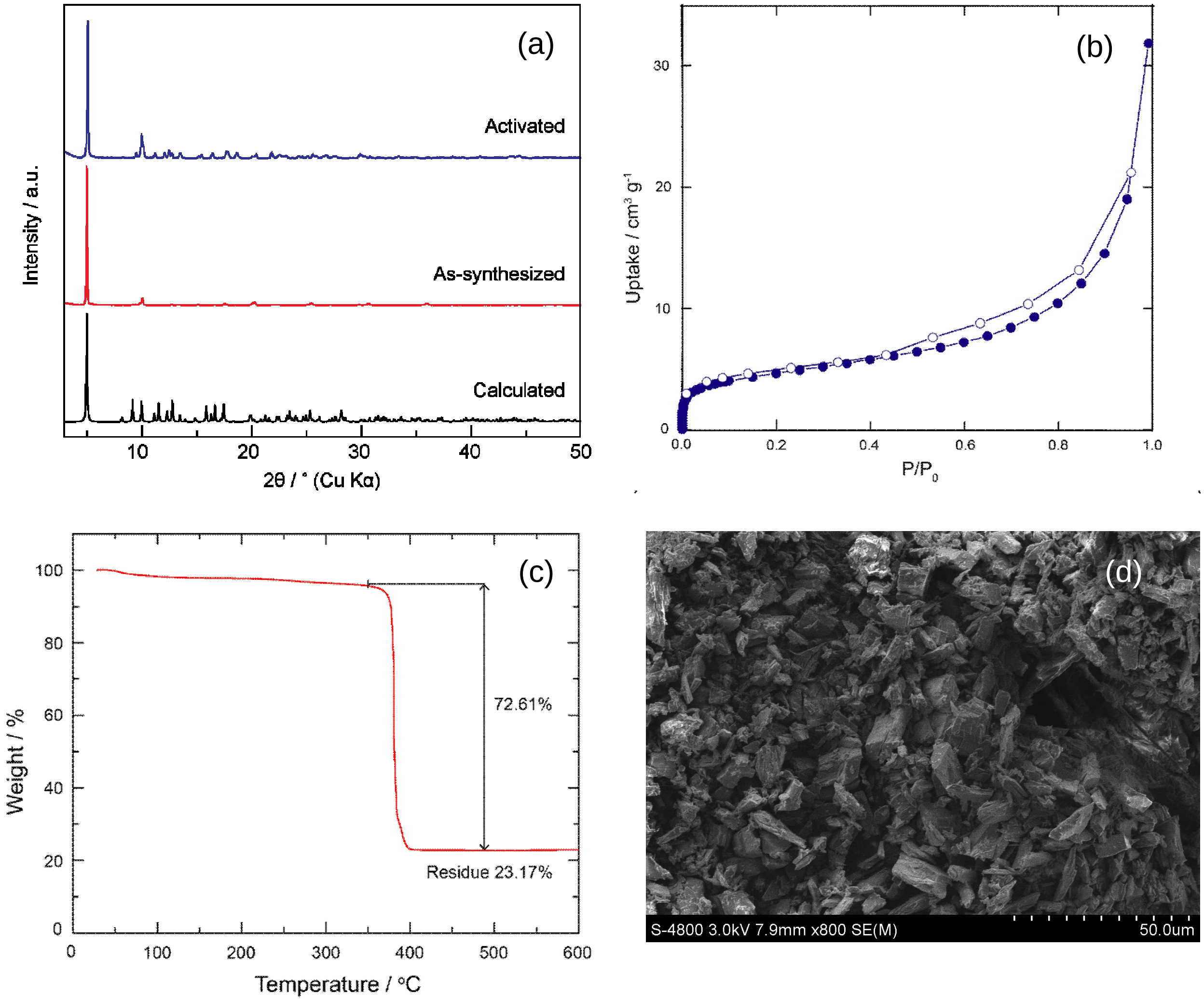

Figure 4. (a) Comparison of the simulated (black) PXRD pattern from the single crystal data with the experimental as-synthesized (red) and activated (blue) PXRD patterns of MOF-589; (b) TGA traces of activated MOF-589 at a heating rate of 5 °C min $^{-1}$ under air flow; (c) N_2 isotherms of MOF-589 at 77 K. Filled and open symbols represent adsorption and desorption branches, respectively. The connecting curves are guides for the eye; (d) SEM image of MOF-589

The permanent porosity of MOF-589 was evaluated by N_2 adsorption isotherms at 77 K using activated material (Figure 4b). As such, MOF-589 exhibited a small N_2 uptake in the low-pressure region. The small amount of adsorbed nitrogen by MOF-589 is largely attributed to the narrow pore size of this material. The resulting N_2 isotherms exhibited typical Type-II behavior, the Brunauer−Emmett−Teller (BET)/Langmuir surface areas for MOF-589 was estimated to be 17/29 m^2 g^{-1}. This measurement is in line with the theoretical accessible surface areas calculated for MOF-589 (72 m^2 g^{-1}, respectively). A hysteresis Type H3 is observed for nonrigid aggregates of plate-like particles. The thermal robustness of MOF-589 was demonstrated by performing thermal gravimetric analysis (TGA) under airflow (Figure 4c). For activated MOF-589, the TGA curve exhibited no appreciable weight loss up to 380 °C, thus highlighting the high thermal stability of this material. The major weight loss observed at ~400 °C in TGA is attributed to framework destruction. Analysis of the residual metal oxide for MOF-589 (23.2%) was found as consistent with the calculated value derived from elemental microanalysis (20.4%). Scanning electron microscopy image analysis indicated the shape homogeneity of synthesized material.

Before investigating the activity of MOF 589 towards Fenton-like reaction, an adsorption–desorption equilibrium between MB and the surface of the MOF 589 was established (Fig. 5). The catalyst (2.0 mg) was soaked and stirred in MB solution (20 ppm and 40 ppm, 1 mL) at room temperature. The result revealed that the equilibrium was reached after first 10 minutes with about 40 % of MB was adsorbed. To obtain better accuracy of the oxidative activity of catalyst, all catalyst was immersed into MB solution for 20 minutes, taken out and rinsed with purified water before being added into decomposition reaction with containing H_2O_2. Therefore, all measurement data were obtained with assumption that impact of adsorption is eliminated.

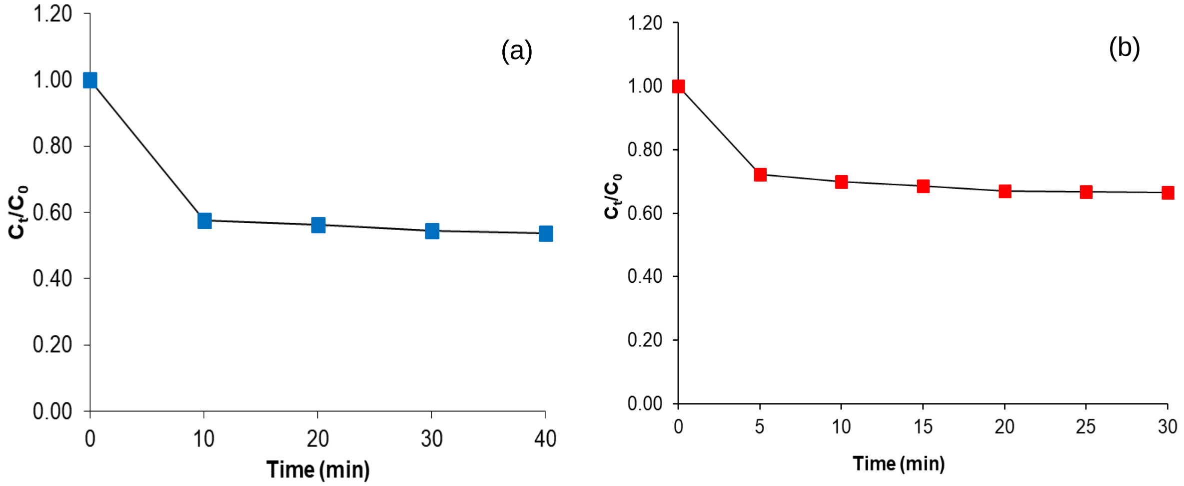

Figure 5. The adsorption–desorption equilibrium between MB and MOF 589.
(a) MB (20 ppm); (b) MB (40 ppm)

The progress of dye deconstruction was monitored using UV-VIS spectrometer. The activity of the catalysts is shown by measuring absorption intensity of MB concentration during the reaction. The optimization screening was investigated with regard to amount of catalyst, MB concentration, and amount of H_2O_2 oxidant (Table 1). In the absence of MOF-589, only 21 % of MB (1 mL, 20 ppm) was decomposed (entry 1) by stoichiometric amount of H_2O_2 . The solution became almost transparent when 1.0 mg of catalyst (1 g/L) was loaded (entry 3). Thus, increasing catalyst amount to 1.5 mg or 2.0 mg is not necessary (entries 4 and 5). Only adsorption occurred without H_2O_2 and optimal results were achieved with 20 µL of the oxidant (entries 6 – 9). Gratifyingly, for more concentrated solution (40 ppm), MOF 589 is still effective with 93 % decomposition of MB (entries 10, 11). Increasing the concentration of dye resulted in moderate drop in activity (entries 12, 13). Notably, only 15 minutes is required for entire process and similar results were obtained when reactions were conducted under inert atmostphere (entries 14 – 16). It is worth mentioning that the optimized condition is the first heterogeneous cerium-based catalytic system for non-photocatalytic degradation of dyes.

Table 1. Optimization of decomposition of methylene blue by H_2O_2 using MOF 589 catalyst

Entry	Amount of catalyst (mg)	Volume of H_2O_2 (µL)	MB concentration (ppm)	GC Yield (%)[a]
1	0	20	20	21
2	0.5	20	20	49
3	1.0	20	20	94
4	1.5	20	20	97
5	2.0	20	20	98
6	1.0	10	20	51
7	1.0	0	20	41
8	1.0	30	20	95
9	1.0	40	20	96
10	1.0	20	30	95
11	**1.0**	**20**	**40**	**93**
12	1.0	20	50	83
13	1.0	20	60	78
14[b]	1.0	20	40	87
15[c]	1.0	20	40	96
16[d]	1.0	20	40	94

[a] MB solution (1 mL), 15 minutes. [b] reaction in 5 minutes. [c] reaction in 30 minutes [d] reaction under argon atmostphere. Kinetic studies of entries and more other information were placed in Supporting Information.

To highlight and gain more insights about catalytic activity of MOF-589, reactions using other previously used catalysts and control experiments were conducted using optimized parameters (Table 2). All solid catalysts were soaked in MB solution, rinsed with purified water, and dried before examining the activity. Surprisingly, iron-based heterogeneous catalytic systems which were frequently employed for Fenton reaction failed to provide sufficient decomposition under tested conditions (entries 1, 2). Magnetic ferrites complexes with other first-row transition metals showed significantly less active (entries 3 – 5). Similar activity were observed with other frequently used Fe-MOFs such as $Fe_3O(BPDC)_3$ and Fe(BTC) (entries 6, 7). Cerium oxide and cerium-exchanged X zeolites provided only 52 % and 32 % yield, respectively (entries 8, 9). In addition, poorer results were achieved with other Ce-MOFs including Ce(BTC), Ce-UiO-66, and Ce-BPDC (entries 10 – 12). We hypothesized that the BIPA-TC linker might have an impact on MOF 589 activity. To gain more clarification, several MOFs of other transition metals using same linker were synthesized and their activity was examined. The results were then compared with MOFs of the identical cluster with different organic linkers. Interestingly, $Co(BIPA\text{-}TC)(H_2O)_3$ and $Ni(BIPA\text{-}TC)(H_2O)_3$ afforded moderately higher efficiency than Co-MOFs and Ni-MOFs using other common linkers such as BDC, BPDC, or BTC (entries 13 – 18). The abovementioned results indicated the cooperative effect of BIPA-TC linker on activity of metal cluster in reaction pathway and this impact is likely more significant in cerium cluster. The hypothesis was supported by the results from reactions using homogeneous counter parts. Specifically, reactions using MOF 589 cluster, $Ce(NO_3)_3.6H_2O$, gave only 48 % decomposition (entry 19) while $CeCl_3$ is less active (entry 20). When only organic linker of MOF 589 was employed, the efficiency was significantly decreased (entry 21).

Table 2. Comparison study with other catalysts

Entry	Type	Catalyst	GC yield (%)	Ref.
1	Heterogeneous iron-based catalysts	Fe_2O_3	40	45
2		Fe_3O_4	57	46
3		$CuFe_2O_4$	39	47
4		$NiFe_2O_4$	49	48
5		$CoFe_2O_4$	64	49
6		$Fe_3O(BDC)_3$	67	

7		Fe(BTC)	52	
8	Other catalysts	CeO_2	52	20
9		Ce-Zeolite X	32	
10		Ce-BTC	23	
11		Ce-UiO-66	41	
12		Ce-BPDC	31	
13		Co(BDC)(DMF)	36	
14		$Co_3(BTC)_2$	48	
15		$Co(BIPA\text{-}TC)(H_2O)_3$	73	
16		Ni(BDC)	30	
17		$Ni(BPDC)(H_2O)_2$	38	
18		$Ni(BIPA\text{-}TC)(H_2O)_3$	71	
19	Homogeneous salts	$Ce(NO_3)_3. 6H_2O$	48	
20		$CeCl_3$	41	
21		H_4BIPA-TC linker	23	

To further confirm the necessity of MOF-589 toward decomposition of MB, control experiments as kinetic study with removal of one reagent were carried out (Figure 6). In the absence of MOF 589, < 20 % of dye was reacted with H_2O_2. Adsorption or/and reaction of fresh MOF 589 with starting material occurred with approximately 33 % yield when H_2O_2 was removed. Comparable results were achieved from reaction conducted in dark indicating that the involvement of light is unlikely.

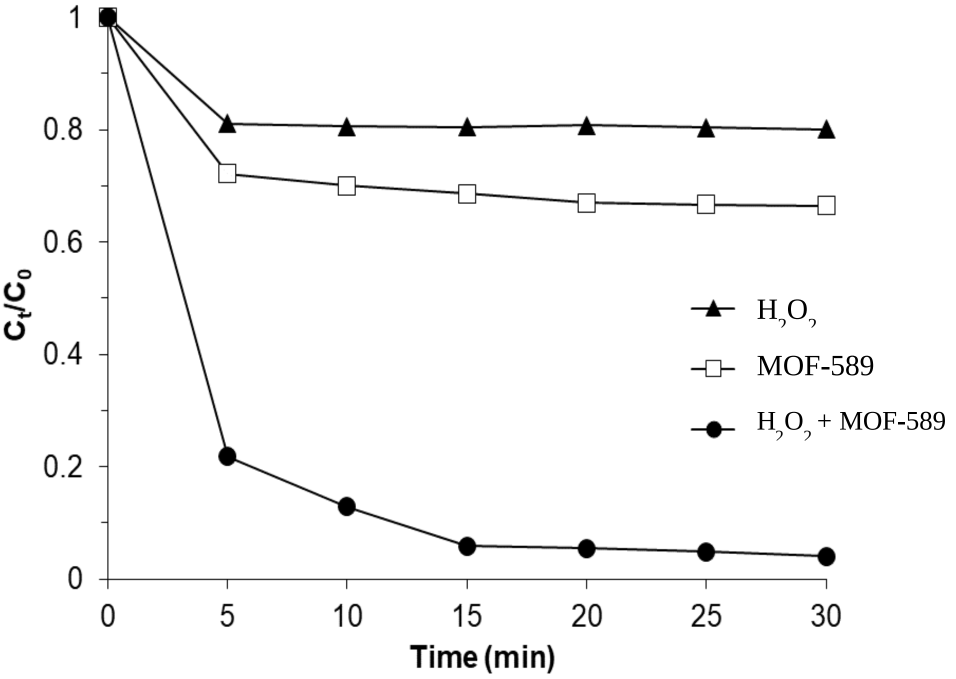

Figure 6. Control experiments

The structural stability of MOF 589 was next investigated by leaching test and recycling study. The experiments were subsequently carried out by repeatedly separating the solid catalyst from the resulting mixture, rinsed with water, and employed for next runs under identical conditions. No significant further decomposition of MB was observed after catalyst was filtered. Inductively coupled plasma - optical emission spectrometry (ICP-OES) measurement of reaction filtrate revealed that the concentration of Ce is < 0.5 ppm. Thus, MB decomposition caused by leached cerium species in the liquid phase is not likely. Subsequently, the MOF 589 could be recovered and reused at least 08 consecutive times with maintained activity. Specifically, a yield of 89 % was still obtained in the 8th run (Figure 7).

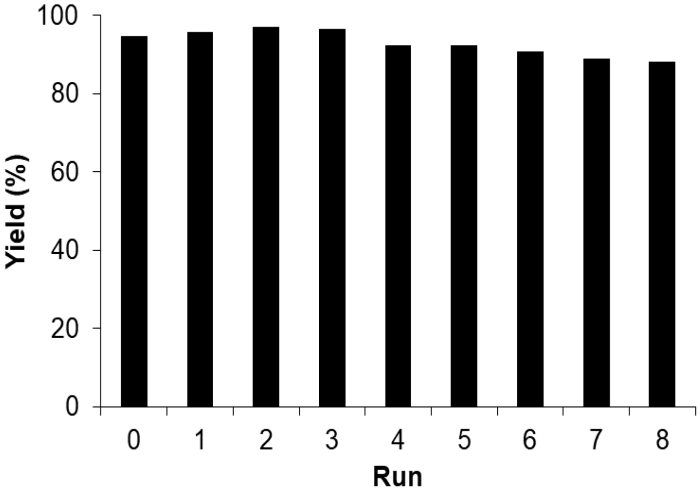

Figure 7. Recycling studies

CONCLUSIONS

In brief, we have reported the synthesis of new lanthanide-based metal-organic framework, namely Ce-MOF-589, by a solvothermal method using benzoimidephenanthroline tetracarboxylic acid as organic linker. Structural and chemo-physical characterization via single crystal and powder X-ray diffraction analysis, thermogravimetrical analysis, scanning electron microscopy, and N_2 adsorption measurement at low pressure and 77 K were presented. Additionally, a catalytic protocol for Fenton-like reaction was developed using this material as an efficient heterogeneous catalyst. The optimized conditions involved the utilization of MOF 589 (1g/L) and H_2O_2 (20 μL) in 15 minutes at room temperature for decomposition of dye solution (1 mL, 40 ppm). Comparison studies revealed the excellent activity of Ce-MOF-589 as compared to other iron-based heterogeneous and cerium-based catalytic systems. Interestingly, preliminary study on structure/activity relationship indicated that cooperative effect of organic linker on metal cluster in reaction pathway is likely. Furthermore, results from leaching test showed that contribution of active leached species is trivial and heterogeneity of MOF 589 was confirmed by its recyclability. Further investigation to clarify the synergetic impact within the MOF structure is currently conducted.

EXPERIMENTAL

Materials and instrumentation

All reagents and starting materials were obtained commercially from Sigma-Aldrich, Merck and were used as received without any further purification unless otherwise noted. Single crystal data were collected on a Bruker D8 Venture diffractometer equipped with Mo Kα radiation (λ= 0.71073 Å) operated at 50 kW and 1.0 mA and PHOTON 100 CMOS detector. Powder X-ray data were collected using a Bruker D8 Advancer employing Ni filtered Cu Kα (λ = 1.54178 Å). The system was also outfitted with an anti-scattering shield that prevents incident diffuse radiation from hitting the detector. Samples were placed on zero background sample holders by dropping powders from a spatula and then leveling the sample with a spatula. The 2θ range was 3-50° with a step size of 0.02° and a fixed counting time of 1 s/step. Solution ^{1}H-NMR and ^{13}C-NMR spectra were acquired on a Bruker Advance II-500 NMR spectrometer. ESI-MS were measured from HPLC, Agilent 1200 Series coupled to MS detector, Bruker micrOTOF-QII. Fourier Transform Infrared (FT-IR) spectra were measured using KBr pellets on a Bruker Vertex 70 system and the output signals are described as: vs, very strong; s, strong; m, medium; sh, shoulder; w, weak; vw, very weak; or br, broad. Thermal gravimetric analysis (TGA) curves were recorded on a TA Q500 thermal analysis system under air flow. Elemental microanalyses (EA) were performed using a LECO CHNS-932 Analyzer. Low pressure N_2 adsorption isotherms were recorded on a Micromeritics 3Flex. A liquid N_2 bath was used for measurements at 77 K and He gas was used to estimate the dead space.

Synthesis of Ce-MOF-589

*Preparation of Benzoimidephenanthroline tetracarboxylic acid (H$_4$BIPA-TC)***:**

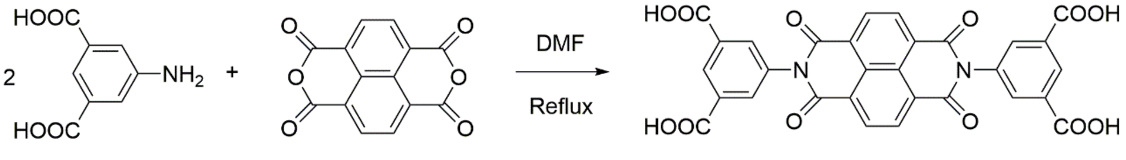

Scheme 1. Synthesis of H$_4$BIPA-TC

H$_4$BIPA-TC was prepared, with slight modifications, according to a previously reported procedure (**Scheme 1**).[41] A 100 mL flask was charged with 5-aminoisophthalic acid (3.639 g, 20 mmol) and 1,4,5,8-naphthalenetetracarboxylic acid dianhydride (2.696 g, 10 mmol). DMF (20 mL) were then added to the mixture and stirred rapidly. The reaction was refluxed for 8 h and then allowed to cool to room temperature. The resulting mixture was filtered over a Buchner funnel and the crude solid was washed thoroughly with cool DMF, H_2O and EtOH. The solid product was then dried in air at 100 ^oC overnight to give yellow compound (84 %, 5.02 g).

Synthesis of MOF-589:

A 0.01 M stock solution of cerium (III) nitrate hexahydrate in deionized water (1 mL) was added to an 8 mL vial. This was followed by the addition of 1 mL solution H_4BIPA-TC in DMA (0.01 M), 1.0 mL of deionized water and CH_3COOH (300 μL) to the mixture, which was subsequently heated at 120 °C for 15 hours, then filtered the hot solution to get the yellow block crystals of MOF-589. As-synthesized sample was washed with DMF (3 × 10 mL) carefully for three days, then immersed in anhydrous ethanol and exchanged three times per day over a period of three days. Then, the solvent was decanted and removed under vacuum at ambient temperature for 24 h, followed by subsequent annealing at 60 ^oC for 24 h to yield activated sample. Elemental Analysis (activated sample): Calculated for $CeC_{30}H_{19}N_2O_{16}$ = $[Ce(HBIPA\text{-}TC)(H_2O)_3]\cdot H_2O$: C, 44.84; H, 2.38; N, 3.49. Found: C, 45.56; H, 2.36; N, 3.49. FT-IR (KBr, 4000–400 cm^{-1}): 3431 (s, br), 1714 (s), 1678 (vs), 1619 (s), 1579 (s), 1553 (w), 1447 (m), 1418 (vw), 1389 (m), 1350 (vs, sh), 1256 (s, sh), 1199 (w), 1120 (w).

Catalytic studies

The catalytic activity of the catalyst was demonstrated by degrading MB in aqueous solution. A vial was charged with 1.0 mL of aqueous MB (40 mg/L) and 1.0 mg of catalyst was added followed by H_2O_2 (20 μL). The reaction mixture was stirred under ambient conditions. At a given time interval, a small quantity of the mixture was pipetted into a quartz cell, diluted 10 times, and its absorption spectrum was measured using an UV-visible spectrophotometer. It is noted that all catalyst was soaked in MB solution in 20 minutes, filtered out, rinsed with purified water and dried before adding into reaction to avoid the consumption of MB via adsorption.

The decomposition of MB was calculated using standard equation (Fig. S3)

Acknowledgements

Vietnam National University – Ho Chi Minh City (VNU-HCM) is acknowledged for financial support via grant No. HS2015-20-01 and INOMAR-CS2018-03. Giao H. Dang and Toan V. Pham are acknowledged the Can Tho University Improvement Project VN14-P6, supported by a Japanese ODA loan.

Keyword: cerium; dye degradation; Fenton reaction; heterogeneous catalysis; metal-organic frameworks.

REFERENCES

1. S. Rangabhashiyam, N. Anu, N. Selvaraju, *J. Environ. Chem. Eng.*, **2013,** *1*, 629-641.
2. J. Sun, S.-P. Sun, G.-L. Wang, L.-P. Qiao, *Dyes and pigm.* **2007**, *74*, 647-652.
3. W. Xiaolong, H. Jingyi, X. Ligang, Z. Qi, *Environ. Pollut.* **2010,** *158*, 1513-1520.
4. W. Epolito, Y. Lee, L. Bottomley, S. Pavlostathis, *Dyes and Pigm.* **2005,** *67*, 35-46.
5. A. Mittal, V. Gajbe, J. Mittal, *J. Hazard Mater.* **2008**, *150*, 364-375.
6. M. Kiel, D. Dobslaw, K.-H. Engesser, *Water Res.* **2014**, *66*, 1-11.
7. X. Lang, W. Ma, C. Chen, H. Ji, J. Zhao, J., *Acc. Chem. Res.* **2013**, *47*, 355-363.
8. S. Caudo, G. Centi, C. Genovese, S. Perathoner, *Top. Catal*, **2006**, *40*, 207-219.
9. D. H. Bremner, R. Molina, F. Martínez, J. A. Melero, Y. Segura, *Appl. Catal. B: Environ.*, **2009**, *90*, 380-388.
10. R. K. Upadhyay, N. Soin, S. S. Roy, *RSC Adv.* **2014**, *4*, 3823-3851.
11. A. Babuponnusami, K. Muthukumar, *J. Environ. Chem. Eng.* **2014**, *2*, 557-572.
12. B. Ensing, F. Buda, E. J. Baerends, *J. Phys. Chem. A*, **2003**, *107*, 5722-5731.
13. M. Antonopoulou, E. Evgenidou, D. Lambropoulou, I. Konstantinou, *Water Res.* **2014**, *53*, 215-234.
14. A. D. Bokare, W. Choi, *J. Hazard. Mater.* **2014**, *275*, 121-135.
15. M. Pereira, L. Oliveira, E. Murad, *Clay Miner.* **2012**, *47*, 285-302.
16. M. Valko, H. Morris, M. Cronin, *Curr. Med. Chem.* **2005,** *12*, 1161-1208.
17. R. S. Ribeiro, A. M. Silva, J. L. Figueiredo, J. L. Faria, H. T. Gomes, *Appl. Catal. B: Environ.* **2016**, *187*, 428-460.
18. P. Nidheesh, *RSC Adv.* **2015**, ***5***, 40552-40577.
19. M. Lu, Y. Zhang, Y. Wang, M. Jiang, X. Yao, *ACS Appl. Mater. Interfaces* **2016**, *8*, 23580 - 23590.
20. E. G. Heckert, S. Seal, W. T. Self, *Environ. Sci. Technol.* **2008**, *42*, 5014-5019.
21. S. S. Lee, W. Song, M. Cho, H. L. Puppala, P. Nguyen, H. Zhu, L. Segatori, V. L. Colvin, *ACS Nano* **2013**, *7*, 9693-9703.
22. S. Parvez, M. J. C. Long, J. R. Poganik, Y. Aye, *Chem. Rev.* **2018**, *118*, 8798-8888.
23. H. Furukawa, K. E. Cordova, M. O'Keeffe, O. M. Yaghi, *Science* **2013**, *341*, 1230444.

24. Y. Lin, C. Kong, Q. Zhang, L. Chen, *Adv. Energy Mater.* **2017**, *7,* 1601296.

25. N. T. Nguyen, H. Furukawa, F. Gándara, H. T. Nguyen, K. E. Cordova, O. M. Yaghi, *Angew. Chem. Int. Ed.* **2014**, *53,* 10645-10648.

26. P. T. Nguyen, H. T. Nguyen, H. N. Nguyen, C. A. Trickett, Q. T. Ton, E. Gutiérrez-Puebla, M. A. Monge, K. E. Cordova, F. Gándara, *ACS Appl. Mater. Interfaces* **2017**, *10,* 733-744.

27. J. N. Hao, B. Yan, *Adv. Funct. Mater.* **2017**, *27,* 1603856.

28. M. H. Teplensky, M. Fantham, P. Li, T. C. Wang, J. P. Mehta, L. J. Young, P. Z. Moghadam, J. T. Hupp, O. K. Farha, C. F. Kaminski, *J. Am. Chem. Soc.* **2017**, *139,* 7522-7532.

29. J. Della Rocca, D. Liu, W. Lin, *Acc. Chem. Res.* **2011**, *44* , 957-968.

30. S. Kaskel, *The Chemistry of Metal-Organic Frameworks, 2 Volume Set: Synthesis, Characterization, and Applications*. John Wiley & Sons: **2016;** Vol. 1.

31. Y.-G. Huang, F.-L. Jiang, M.-C. Hong, *Coord. Chem. Rev.* **2009**, *253,* 2814-2834.

32. S. Roy, A. Chakraborty, T. K. Maji, *Coord. Chem. Rev.* **2014**, *273,* 139-164.

33. M. V. Marinho, D. O. Reis, W. X. Oliveira, L. F. Marques, H. O. Stumpf, M. Déniz, J. Pasán, C. Ruiz-Pérez, J. Cano, F. Lloret, *Inorg. Chem.* **2017**, *56*, 2108-2123.

34. X.-Z. Song, S.-Y. Song, H.-J. Zhang, Luminescent Lanthanide Metal–Organic Frameworks. In *Lanthanide metal-organic frameworks*, Springer: **2014**, 109-144.

35. Z. Guo, H. Xu, S. Su, J. Cai, S. Dang, S. Xiang, G. Qian, H. Zhang, M. O'Keeffe, B. Chen, *Chem. Commun.* **2011**, *47,* 5551-5553.

36. M. Allendorf, C. Bauer, R. Bhakta, R. Houk, *Chem. Soc. Rev.* **2009**, *38,* 1330-1352.

37. L. Meyer, F. Schönfeld, A. Zurawski, M. Mai, C. Feldmann, K. Müller-Buschbaum, *Dalton Trans.* **2015**, *44*, 4070-4079.

38. D. Yue, D. Zhao, J. Zhang, L. Zhang, K. Jiang, X. Zhang, Y. Cui, Y. Yang, B. Chen, G. Qian, *Chem. Commun.* **2017**, *53*, 11221-11224.

39. R. Dalapati, B. Sakthivel, M. K. Ghosalya, A. Dhakshinamoorthy, S. Biswas, *CrystEngComm* **2017**, *19*, 5915-5925.

40. K. Binnemans, *Chem. Rev.* **2009,** *109*, 4283-4374.

41. A. J. Cairns, J. A. Perman, L. Wojtas, V. C. Kravtsov, M. H. Alkordi, M. Eddaoudi, M. J. Zaworotko, *J. Am. Chem. Soc.* **2008**, *130*, 1560-1561.

42. V. A. Blatov, A. P. Shevchenko, D. M. Proserpio, *Cryst. Growth Des.* **2014**, *14*, 3576-3586.

43. A. L. Spek, *Acta Crystallogr. D: Biol. Crystallogr.* **2009**, *65*, 148-155.

44. V. Robins, S. Ramsden, S. Hyde, In *EPINET: euclidean patterns in non-euclidean tilings*, ACM SIGGRAPH 2006 Research posters, ACM: 2006; p 95.

45. N. Panda, H. Sahoo and S. Mohapatra, *J. Hazard. Mater*. **2011**, *185*, 359–365.

46. L. J. Xu, J. L. Wang, *Appl. Catal. B* **2012**, *123*, 117–126.

47. Q. Qin, Y. Liu, X. Li, T. Suna, Y. Xu, *RSC Adv.* **2018**, *8*, 1071–1077.

48. Z. Chen, Y. Gao, D. Mu, H. Shi, D. Lou, S.-Y. Liu, *Dalton Trans.* **2019**, *48*, 3038-3044.

49. A. Kalam, A. G.Al-Sehemi, M. Assiri, G. Du, T. Ahmad, I. Ahmad, M.Pannipara, *Results in Physics* **2018**, *8*, 1046–1053